Storylines of Sahel precipitation change: roles of the North Atlantic and Euro-Mediterranean temperature

Paul-Arthur Monerie[1], Michela Biasutti[2], Juliette Mignot[3], Elsa Mohino[4], Benjamin Pohl[5], Giuseppe Zappa[6]

[1] National Centre for Atmospheric Science, Reading, United Kingdom

[2] Lamont-Doherty Earth Observatory of Columbia University, Palisades, NY, USA

[3] LOCEAN/IPSL Sorbonne University/IRD/CNRS/MNHN, Paris, France

[4] Dpto. Física de la Tierra y Astrofísica, Facultad Ciencias Físicas, Universidad Complutense de Madrid, Ciudad Universitaria, Plaza Ciencias, 28040 Madrid, Spain

[5] Centre de Recherches de Climatologie, UMR 6282 Biogéosciences, CNRS/Université de Bourgogne Franche-Comté, Dijon, France

[6] National Research Council of Italy, Institute of Atmospheric Sciences and Climate (CNR-ISAC), Bologna, Italy

Key Points

- Future changes in Sahel precipitation are uncertain

- Uncertainties in changes in North Atlantic and in Euro-Mediterranean temperatures explain up to 50% of the central Sahel precipitation change uncertainty

- Uncertainty in changes in Sahel precipitation is associated with uncertainty in the future northward shift of the Saharan heat low

Abstract

Future changes in Sahel precipitation are uncertain because of large differences among projections from various models. In order to explore this uncertainty, we use a storyline approach which seeks to identify alternative plausible evolutions of Sahel precipitation and their driving factors. By analysing projections from the CMIP6 climate models, we show that changes in North Atlantic and in Euro-Mediterranean temperatures explain up to 50% of the central Sahel precipitation change uncertainty. We then construct several storylines of Sahel precipitation change based on future plausible changes in North Atlantic and Euro-Mediterranean temperatures. In one storyline, an amplified warming of both the North Atlantic and the Euro-Mediterranean areas promotes a northward shift of the West African monsoon, increasing precipitation over the central Sahel, while, in another storyline, a moderate warming in both regions is associated with a small change in precipitation over the central Sahel and a decrease in precipitation over the western Sahel, at the end of the 21st century. These results indicate that reducing uncertainty in future changes in Sahel precipitation could be achieved by reducing uncertainty in the future warming of the North Atlantic and the Euro-Mediterranean areas.

Plain Language Summary

Variations in the strength of the West African Monsoon (WAM) circulation has societal impacts on around 80 million people from Senegal to Chad. However, future projections of the WAM precipitation are uncertain for the end of the 21st century because of strong differences from a climate model to another. We show here that sources of uncertainty in Sahel precipitation depend on changes in North Atlantic and Euro-Mediterranean temperature, relative to changes in global mean surface air temperature. We show that differences between climate models at simulating the future warming over the North Atlantic and Euro-Mediterranean area allows explaining a large proportion of the uncertainty in precipitation change over the central Sahel. We provide a method that could be helpful at selecting models for impacts studies, selecting models based on their sensitivity to climate change over the North Atlantic and Mediterranean Sea.

1. Introduction

The West African Monsoon (WAM) brings precipitation in summer for around 80 million people from Senegal to Chad. Variability of the monsoon circulation has large impacts on Sahelian societies: on human health (Ramin et McMichael 2009; Jankowska et al. 2012; Cissé 2019), agropastoral activities (Marega et al. 2018), agriculture (Sultan et Gaetani 2016), and the gross domestic product (Sainte Fare Garnot et al. 2018; Baarsch et al. 2020), among others. Therefore, understanding, predicting, and projecting current and future variations of precipitation across the Sahel is an issue of major importance.

Precipitation has increased over the Sahel since the drought of the 1970s and 1980s (Sanogo et al. 2015). The current understanding attributes the recovery to a combination of factors: a warming of the North Atlantic (Martin et Thorncroft 2014) and Mediterranean (Park et al. 2016) Sea Surface Temperature (SSTs), an increase in greenhouse gas (GHG) emissions (Dong et Sutton 2015; Monerie et al. 2022), and a decrease in anthropogenic aerosol emissions from Europe and northern America (Marvel et al. 2020; Hirasawa et al. 2020; Monerie et al. 2022). The future evolution in GHG atmospheric concentration is uncertain (O'Neill et al. 2016). Yet, GHG concentrations are projected to increase until the end of the 21st century in most of the emission scenarios considered in the IPCC AR6. We thus expect Sahel precipitation to be primarily affected by future changes in GHG concentrations via their effects on surface air temperature and atmospheric circulation.

Multi-model mean projections show an increase in precipitation over the central Sahel and a decrease in precipitation over the Western Sahel (Biasutti 2013a; Monerie et al. 2020b). This zonal contrast in precipitation change arises from the competitive roles of increases in land surface and sea surface temperature (Biasutti 2013b; Gaetani et al. 2017; Monerie et al. 2020a, 2021). Future changes in Sahel precipitation are nevertheless very model dependent in both ensembles of the 5th and 6th phases of the Climate Model Intercomparison Project (CMIP5 and CMIP6; Taylor et al. 2012; Eyring et al. 2016). The inter-model spread in precipitation change is higher than the multi model mean change itself over a large part of West Africa (Monerie et al. 2020b) implying that even the direction of change is uncertain. Uncertainty in Sahel precipitation change primarily comes from differences among climate models in their projected atmospheric circulation patterns (Monerie et al. 2020b), and to uncertainty in future changes of the West African monsoon circulation tied to uncertainty in the simulation of the increase in atmospheric temperature over the northern Hemisphere, over both land and ocean (Park et al. 2015; Monerie et al. 2021). Among the different oceanic regions over the northern Hemisphere, the uncertainty in Sahel precipitation was especially tied to that over the Mediterranean SSTs in sensitivity experiments by Park et al. (2016) when they imposed increases of different magnitudes in temperature over the northern Hemisphere and for several oceanic basins, separately under the same climate model. They showed that the warming of the North Atlantic Ocean also contribute to the increase in Sahel precipitation.

In addition to simulating different patterns in SST, CMIP6 climate models simulate a large range of changes in global mean surface air temperature (O'Neill et al. 2016). Yet, Monerie et al. (2020b) showed that the inter-model spread in global mean surface temperature only explains a small proportion of the inter-model spread in Sahel precipitation change.

Because of strong uncertainty, projections of future changes in Sahel precipitation do not provide useful and reliable information to the decision makers developing adaptation strategies in the region. Within the ultimate goal of reducing uncertainty, we aim at improving our understanding of drivers of Sahel precipitation, focusing on mechanisms that explain differences among models' projections. Previous works suggested that uncertainty in Sahel precipitation is primarily due to how models simulate future changes of the atmospheric circulation. We hence hypothesis that we can document sources of Sahel precipitation uncertainty focusing on drivers of the West African monsoon circulation.

We use a storyline approach (Zappa et Shepherd 2017) to document and represent uncertainty in future changes in Sahel precipitation. This is done by developing storylines, akin to response scenarios for a given forcing, that span the projections from an ensemble of climate models and that provide physically self-consistent future evolutions of global and regional climate. The basis for the construction of these storylines are the remote drivers of the circulation response. The storyline approach has been applied to Europe (Zappa et Shepherd 2017) and several regions of the southern hemisphere (Mindlin et al. 2020). Here, we apply it to future changes in precipitation over the Sahel, targeting the projections by a large number of CMIP6 models under one emission scenario. In Section 2, we introduce the dataset used in this paper, detail the indices used to represent the Sahel changes and its possible drivers, and provide a succinct introduction to the implementation of the storyline approach and to the decomposition of precipitation into thermodynamically and dynamically forced components. In Section 3, we motivate the selection of the Euro-Mediterranean and North Atlantic surface temperature regional means as the remote drivers of the West African monsoon on which the storylines are constructed. In Section 4 we construct the storylines and show the range of projections that can be encompassed by chosen warming levels for each drivers. Section 5 introduce the alternative approach of spanning the uncertainty by choosing subsets of the CMIP6 ensemble based on where they lay in the phase space of drivers' warming and we confirm that the range of Sahel precipitation response is explained by a range of circulation responses. We conclude the paper with a short summary and discussion.

2. Data and Methods

2.1 Simulations

We use historical and scenario simulations from 43 ocean–atmosphere coupled general circulation models (AOGCMs) that participated to CMIP6 (Table S1). The historical simulations cover the 1850-2014 period and are forced by recontructions of external forcings, *e.g.*, greenhouse gases, anthropogenic aerosols, solar cycle, volcanic activity over the historical period (Eyring et al. 2016). For the 2015-2100 period, we use the SSP5-8.5 high-emissions scenario (O'Neill et al. 2016), in which GHG emissions lead to a radiative imbalance at the top of the atmosphere of approximately 8.5 $W.m^{-2}$ at the end of the 21st century. We have used one ensemble member for each model, relying on the fact that uncertainty in the Sahel response by 2100 is massively explained by differences between climate models, rather than internal variability (Monerie et al. 2020b).

The effect of climate change is assessed by comparing precipitation and temperature of the late 21st century (period 2060-2099) to the late 20th century (1960-1999). The 1960-1999 historical period is chosen to sample both the drought of the 1970s-1980s and the wettest 1960s. We use summer-mean (from July to September, JAS) anomalies.

2.2 Indices

Because we focus on the uncertainty created by the pattern of warming, all indices are scaled by defined as the change in global mean surface air temperature (ΔT) over the same periods amd simulated by each model. Below we detail the regional means defining individual indices.

2.2.1 Sahel precipitation

As explained above, multi-model mean estimates of future changes in Sahel precipitation project onto a zonal contrast in precipitation change (Monerie et al. 2020a), with a decrease in precipitation over the western Sahel and an increase in precipitation over the central Sahel. We define two precipitation indices to account for this regional heterogeneity in precipitation change. The western Sahel precipitation index is obtained by averaging precipitation between 20°W and 5°W, and from 10°N to 20°N. The central Sahel precipitation index is defined as the average of precipitation between 5°W and 20°E and between 10°N and 20°N, as in Monerie et al. (2020a).

2.2.2 Temperature indices

The choice of the remote drivers of uncertainty in Sahel precipitation change analysed here are motivated by previous studies on the drivers of the west African monsoon discussed in the introduction, and by the analyses presented in Figure 1, discussed in Sect. 3. Unless specificed differently, averages are computed over both oceanic and land areas. These drivers are defined as:

- The North Atlantic Ocean (NATL), as inferred from a regional index of the surface air temperature, from 60°W to 0°E and from 20°N to 60°N, considering ocean grid points only. The change in this index from the late 20th Century to the late 21st Century is denoted as ΔT_{NATL}.
- The Euro-Mediterranean region (MED), defined as the average of the surface air temperature from 0°E to 40°E and from 30°N to 50°N. Its change is denoted as ΔT_{MED}.
- The inter-hemispheric temperature gradient, defined as the difference between the area-averaged temperature between the northern hemisphere (0°N-87.5°N) and the southern hemisphere (87.5°S-0°N).

- The northern hemisphere temperature relative to the tropics, defined as the difference between the mean surface air temperature in 20°N-75°N relative to the mean in 20°S-20°N (Park et al. 2015).
- The northern Pacific surface air temperature, which is the area average from 30°N to 60°N and from 150°E to 240°E, considering ocean grid points only.
- The polar amplification, defined as the polar cap mean in 60°N-90°N, following Manzini et al. (2014).
- The temperature of the Saharan desert, defined between 20°N and 30°N and between 30°W and 30°E, over land only.

2.2.3 Location of the Saharan Heat Low

Meridional shifts of the Saharan Heat Low (SHL) have strong effects on Sahel precipitation, with a northward shift of the SHL typically associated with an increase in Sahel precipitation (Lavaysse et al. 2009; Shekhar et Boos 2017).

We define an index that documents the meridional location of the SHL. The index is based on the low-level atmospheric thickness (LLAT; Lavaysse et al. 2009), that is the difference between geopotential height (Z) at 700 hPa and 925 hPa (*i.e.*, LLAT = Z700 – Z925). The latitudinal location of the SHL is then defined as the latitudinal location of the maximum of the LLAT sector zonal mean. We only consider LLAT values that lie between 15°W and 30°E and from 0°N to 40°N. We smooth the LLAT values performing a cubic splines interpolation before defining the latitudinal location of the SHL (Shekhar et Boos 2017).

2.3 Storyline approach

We estimate the epochal change for a given field *V* with a pattern scaling approach following (Zappa et Shepherd 2017): for a location *x* and a model *m*:

$$\Delta V_{xm} = \Delta T_m R_{xm} \quad (1)$$

Where, ΔT is the change in global mean surface air temperature and *R* the climate response pattern.

The pattern R_{xm} is then modelled as a linear combination of the response to a number of remote drivers, scaled by ΔT and standardized. Given a pair of remote drivers, as in this study, we estimate R_{xm} as follows:

$$R_{xm} = a_x + b_x\left(\frac{\Delta T_{Driver1}}{\Delta T}\right)'_m + c_x\left(\frac{\Delta T_{Driver2}}{\Delta T}\right)'_m + e_{xm} \quad (2)$$

where primes (‘) indicate that the changes of the remote drivers are standardized using the CMIP6 ensemble mean and standard deviation. The coefficients a_x, b_x, and c_x are obtained using a multiple linear regression across the model ensemble. With this fit, a_x is the response that is expected with no change of the drivers with respect to the multi model mean. b_x, and c_x are the sensitivity of R_{xm} to the response to anomalies with respect to the multi-model mean of the two remote drivers, scaled by ΔT, respectively. e_{xm} is the residual that is not captured by the linear expansion and is associated with changes that are due to external forcing and effect of internal climate variability, but that are not associated with the response of the two remote drivers.

From equations (1) and (2), the change of a given field, per ΔT, is finally obtained as:

$$\frac{\Delta V_{xm}}{\Delta T_m} = a_x + b_x(\frac{\Delta T_{Driver1}}{\Delta T})'_m + c_x(\frac{\Delta T_{Driver2}}{\Delta T})'_m + e_{xm} \quad (3)$$

2.4 Decomposing precipitation anomalies

We estimate the thermodynamic and dynamic components of precipitation change following Chadwick et al. (2013). The decomposition method assumes that precipitation is primarily convective in the tropics and that precipitation can be approximated by,

$P = M^* q$ and thus $\Delta P = \Delta(M^* q)$ (4)

Were *P* is precipitation, *M** is a proxy for convective mass flux, from the boundary layer to the free troposphere, and *q* is near-surface specific humidity. *P*, *M** and *q* are computed for each grid pont, with Mstar obtained from model data as P/q. Δ indicates the epochal change in precipitation, as defined in Sect. 2.2. An increase in precipitation is associated with either an increase in near-surface specific humidity, a strengthening of the convective mass flux, or both. We can then reformulate precipitation change in terms of thermodynamic (ΔP_{therm}), dynamic (ΔP_{dyn}) and cross nonlinear (ΔP_{cross}) components.

$$\Delta P = M^* \Delta q + q \Delta M^* + \Delta q \Delta M^* \quad (5)$$

In other words,

$$\Delta P = \Delta P_{therm} + \Delta P_{dyn} + \Delta P_{cross} \quad (6)$$

Sahel precipitation change uncertainty is primarily due to ΔP_{dyn} (Monerie et al. 2020b), which we can decompose into an anomaly associated with the effect of climate change on a future weakening of the large-scale tropical circulation ΔP_{weak}, and with a change in the pattern of the circulation ΔP_{shift}, following (Chadwick et al. 2016), as,

$$\Delta P_{dyn} = \Delta P_{weak} + \Delta P_{shift} \quad (7)$$

Where

$$\Delta P_{weak} = q \Delta M^*_{weak} \quad (8)$$

And

$$\Delta P_{shift} = q \Delta M^*_{shift} \quad (9)$$

ΔM^*_{weak} is the change in mass flux that is associated with a change of the strength of the mean tropical circulation. Chadwick et al. (2013) and (Held et Soden 2006) show that this change is proportional to the climatological mass-flux field, and thus,

$$\Delta M^*_{weak} = -\propto M^* \quad (10)$$

With

$$\propto = -(tropical\ mean\ \Delta M^* / tropical\ mean\ M^*) \quad (11)$$

The tropical mean is here the average between 30°S and 30°N.

Finally, ΔM^*_{shift} is computed as the residual between ΔM^* and ΔM^*_{weak}:

$$\Delta M^*_{shift} = \Delta M^* - \Delta M^*_{weak} \quad (12)$$

The decomposition is performed using monthly means prior to computing the seasonal means and before averaging over the 40 years period.

3. Drivers of uncertainty in Sahel precipitation change

Figure 1 shows the regression coefficient of the changes in surface air temperature against the changes in summer Sahel precipitation for the end of the 21st century, across CMIP6 models. Simulated uncertainty in changes in western and central Sahel precipitation is associated with uncertainty in future changes in temperature over the northern Hemisphere, as shown in Park et al. (2015). This pattern of SST is different from the one typically associated with the observed variations of Sahel precipitation at seasonal to multi-decadal scales. The latter shows larger anomalies in the tropical oceans and subsumes the influence of ENSO in the East Pacific, the dipole mode in the Atlantic, and the interhemispheric gradient. In contrast, Figure 1 shows that larger projected warming over the North Pacific, North Atlantic, Mediterranean, Arctic temperature, and over northern Africa and Europe is associated with a greater degree of Sahel wetting in simulations of the 21st century.

Within the large region identified by the regression analysis as causing disagreement across the CMIP6 models, we select two sub-regions to function as Sahel drivers in the storyline approach based on the following criteria. First, they have a strong effect on Sahel precipitation, as identified in the literature from observed statistics and from modelling studies that provide a mechanistic explanation. Second, their variations across models are, as much as possible, independent; this is necessary in order to span as much inter-model variations as possible with the least number of drivers.

The first criterion leaves as possible choices the North Atlantic and the Euro-Mediterranean area, which are correlated to the Sahel in observations (Rowell 2003; Giannini et al. 2013) and have been shown to affect the temperature and humidity advected into the monsoon region (Liu et al. 2014), and the extra-tropical zonal mean, which has been linked to the energetic imbalance that shifts the ITCZ (*e.g.*, Schneider et al. 2014). The same criterion leads us to exclude the Norh Pacific and the Arctic, which have not been linked to Sahel precipitation variability other than by their contribution to the interhemispheric gradient. The surface temperature over North Africa has been invoked as a possible driver of Sahel precipitation through its effect on the Sahara Heat Low (Lavaysse et al. 2009; Mutton et al. 2022), but the correspondence between the Saharan temperature and the Sahel is weak (Biasutti et al. 2008, Figure 2), leading us to exclude it from the candidate list.

The second criterion — selecting drivers with a low co-variability in order to explore the widest possible range of sources of uncertainty for Sahel precipitation change — is checked by computing cross-correlations between each pair of indices (Figure 2). Among the candidate indices, the two drivers that exhibit the weakest correlation coefficient with each other are the north Atlantic and the Euro-Mediterranean warming. The inter-model correlation between $\frac{\Delta T_{NATL}}{\Delta T}$ and $\frac{\Delta T_{MED}}{\Delta T}$ is 0.35 (Figure 2) indicating that only ~12% of the temperature variance across models is not independent in the two regions.

Drivers other than surface temperature could be selected, such as the Sahara Heat Low. Climate change leads to a northward shift of the SHL (*e.g.*, Monerie et al. 2020, among others), favouring an increase in precipitation over the Sahel (Biasutti et al. 2009; Roehrig et al. 2011; Lavaysse et al. 2016; Shekhar et Boos 2017) (Figure 2). Indeed, the uncertainty in the simulated change in the latitude of the SHL is highly correlated with the uncertainty in Sahel precipitation both in the West and the Central Sahel (Figure 2). Yet, this quantity is well correlated with all the relevant indices (correlation coefficient between $\frac{\Delta SHL_{loc}}{\Delta T}$ and $\frac{\Delta T_{MED}}{\Delta T}$ is r=0.72 and correlation coefficient between $\frac{\Delta SHL_{loc}}{\Delta T}$ and $\frac{\Delta T_{NATL}}{\Delta T}$

is r=0.57, both significant at the 1% level) and therefore it is not conducive to creating the two-dimensional regression that we are seeking (*i.e.*, it does not match our second criterion). Moreover, it is still unclear if the location of the SHL ought to be considered an external driver to Sahel precipitation, or if it is part of a tightly coupled system. For these reasons, we do not select the uncertainty in the location of the SHL for the storyline approach. Our choice, instead, is to select the North Atlantic and Euro-Mediterranean temperature indices as drivers and assume that the effect of uncertainty in future changes in the location of the SHL is already included in the ensuing scenarios, given that these drivers affect the Sahel by shifting the SHL northwards (Rowell 2003; Martin et Thorncroft 2014).

The inter-model spread in temperature change is high over the North Atlantic Ocean with projections ranging from a decrease to an increase in temperature over the Atlantic subpolar gyre (Swingedouw et al. 2021). The positive regression coefficients over this region in Figure 1 are consistent with previous results highlighting the significant influence of North Atlantic SSTs anomalies, as the ones related to the Atlantic Multidecadal Variability (AMV), on Sahel precipitation (*e.g.*, Mohino et al. 2011). A positive phase of the AMV, *i.e.*, a warmer than usual North Atlantic ocean, is indeed associated with anomalously high precipitation over the Sahel, and conversely in both observations and simulations (Mohino et al. 2011; Monerie et al. 2019). A possible role of the North Atlantic SSTs in future changes in Sahel precipitation was established in previous work (Park et al. 2016; Monerie et al. 2020b; Bellomo et al. 2021; Swingedouw et al. 2021). We confirm here, using a multiple linear regression framework, that models that simulate the strongest warming of the North Atlantic Ocean, relative to the global mean surface temperature change, also simulate stronger increases in Sahel precipitation (Figure 3a).

Anomalously high temperature of the Mediterranean Sea is also associated with an increase in Sahel precipitation, in both observations and simulations (Rowell 2003; Fontaine et al. 2010). The warming of the Mediterranean Sea is associated with a warming of the Sahara desert (Figure S1) and a strengthening of the northerly moisture flux (Rowell 2003) that allow Sahel precipitation to increase. Warming of the Mediterranean Sea, due to climate change, was also found to be associated with an increase in precipitation over the Sahel (Park et al. 2016). Figure 3b confirms that changes in Sahel precipitation are sensitive to the increase in temperature over the Euro-Mediterranean region.

We note that Figure 1 shows negative regression coefficient over the Sahel, which is consistent with precipitation affecting local surface temperature: enhanced Sahel precipitation cools the surface through increased moisture availability and enhanced latent heat flux and through an enhanced cloud cover that reduces net surface shortwave radiation.

4. Uncertainty due to the remote drivers

4.1 Constructing the scenarios

We express uncertainty in changes in precipitation as a function of uncertainty in changes in North Atlantic and Euro-Mediterranean surface air temperature (Equation 3). We show that this framework allows explaining up to 50% of the uncertainty in precipitation change of the CMIP6 ensemble (Figure 4). We then explore the uncertainty associated with the drivers, by constructing different storylines of Sahel precipitation change depending on the changes in North Atlantic and Euro-Mediterranean temperature.

The effects of anomalously high and low warming of the North Atlantic and Euro-Mediterranean regions on a variable *V* are defined using the regression coefficients from Equation (2) and displayed in Figure 3, b_x for the North Atlantic and c_x for the Euro-Mediterranean area.

The scenarios are then constructed using a scenario index *i*, following Zappa and Shepherd (2017), as:

$$\frac{\Delta V_x}{\Delta T} = a_x \pm ib_x \pm ic_x \quad (13)$$

Figure 5 shows the change in North Atlantic ($\frac{\Delta T_{NATL}}{\Delta T}$) and Euro-Mediterranean ($\frac{\Delta T_{MED}}{\Delta T}$) surface air temperature, scaled by changes in global mean surface air temperature, for each CMIP6 climate model. There is a large inter-model spread in both drivers (Figure 5). We show that the North Atlantic warming can be faster or slower than global mean warming, while the Euro-Mediterranean area can warm up to twice as fast as the global mean warming. We then construct four extreme, but plausible, storylines of Sahel precipitation change, with each reflecting different combinations of future warming of the North Atlantic and Euro-Mediterranean areas.

To account for the weak correlation between the two indices (r=0.35), we define the scenario index following Mindlin et al. (2020) (See the Supplementary Material). This approach implies using a different scenario index for the high scenarios (A+M+ and A-M-) and the intermediate scenarios (A+M- and A-M+), with,

$$i = i_1, \text{ and}$$
$$i_1 = \sqrt{\frac{(1-r^2)}{2(1-r)}\chi^2(0.8; 2)} \sim 1.46 \quad (14)$$

for A+M+ and A-M-, and,

$$i = i_2, \text{ and}$$
$$i_2 = \sqrt{\frac{(1-r^2)}{2(1+r)}\chi^2(0.8; 2)} \sim 1.01 \quad (15)$$

for A+M- and A-M+.

χ^2 (k,p) is the quantile function of the chi-squared distribution with k degrees of freedom evaluated at probability p. The values are chosen so that the anomalies in the two driver responses are selected to lie on the 80% confidence region of the joint CMIP6 distribution (see for instance Figure 5 for the temperature indices).

A+M+ is the scenario for which North Atlantic and Euro-Mediterranean temperatures increase more strongly than the global mean surface air temperature, and relative to the CMIP6 ensemble mean (Table S2). A-M- is the opposite scenario, for which North Atlantic and Euro-Mediterranean temperatures increase more weakly than the ensemble-mean. A+M- and A-M+ are the scenarios where North Atlantic temperature increases strongly and Euro-Mediterranean temperature increases weakly, and vice versa, all relative to the increase in global mean surface air temperature and to the CMIP6 ensemble. Figure 5 shows that all four scenarios lie within the CMIP6 ensemble spread and are thus associated with plausible changes in North Atlantic and Euro-Mediterranean temperature.

4.2 Effects of the scenarios on changes in precipitation

Figure 6a shows the effect of climate change, scaled by ΔT, on precipitation. The multi-model mean forced response is associated with an increase in precipitation over the central Sahel and a small decrease in precipitation over the western Sahel (Figure 6a), as shown in Monerie et al. (2020b), among others. The pattern of precipitation change indicates that the monsoon is projected to strengthen and shift northward towards the end of the 21st century over the central Sahel and to weaken and to shift southward over the western Sahel and the tropical Atlantic Ocean (Figure 6a).

The A+M+ scenario shows a stronger increase in precipitation over land than the multi-model mean. The decrease in western Sahel precipitation is considerably reduced and it largely turns into a wetting of the region (Figure 6b). In contrast to the multi-model mean, the South-North dipole in precipitation indicates that the West African monsoon strengthens and shifts northward, over land and over the tropical Atlantic Ocean (Figure 6b). In A-M-, no change in precipitation is found over the central Sahel, while precipitation decreases strongly over the western Sahel. The two opposite scenarios thus have strong impacts on Sahel precipitation change, with A+M+ and A-M- portraying different futures: a substantial increase in precipitation in the former and an increase in the likelihood of drought conditions in the latter.

Uncertainties in changes in North Atlantic and Euro-Mediterranean temperature are associated with similar uncertainty (both in intensity and sign) in Sahel precipitation (Figure 3a and Figure 3b). As a result, a scenario with a high increase in Atlantic temperature and a low increase in Euro-Mediterranean temperature (A+M-) shows changes in precipitation that are similar to both the ensemble mean (Figure 6a and Figure 6d) and to the A-M+ storyline (Figure 6d and Figure 6e).

We show that the four scenarios as defined above allow sampling uncertainty in Sahel precipitation change at the end of the 21st century (Figure 7a). A+M- and A-M+ show results that are close to the CMIP6 multi-model mean, and A+M+ and A-M- are extreme scenarios but are not outliers, since these scenarios lie within the CMIP6 distribution (Figure 7a). A+M+ and A-M- are plausible scenarios in precipitation change for the end of the 21st century and provide the strongest difference to the multi model mean. In the remainder of the study we then mostly focus on A+M+ and A-M- scenarios.

4.3 Time evolution of the changes in Sahel precipitation

We now assess the effects of the two selected scenarios on the time-evolving changes in Sahel precipitation, across both the 20th and the 21st centuries. This is done by using Equation (13) but as a function of ΔT:

$$\Delta V_x = \Delta T[a_x \pm i(b_x \pm c_x)] \qquad (16)$$

The scenario index *i*, and the regression coefficients a_x, b_x and c_x are kept constant. We obtain a time evolution of ΔV_x, using Equation 16 and with ΔT that varies from one year to another. We computed changes in precipitation for each grid point before deriving the western and central precipitation indexes. We show that the CMIP6 western and central Sahel precipitation change distribution (ensemble-mean and ensemble spread) does not fall well between the A+M+ and A-M- scenarios before the mid-21st century (Figure 7b and Figure 7c), showing limitations in this reconstruction of the time-evolution of Sahel precipitation change.

We assume the inability of the scenarios to capture the early 21st century CMIP6 Sahel precipitation change uncertainty to be an inherent issue of the pattern scaling method we use. We test this hypothesis by trying to reconstruct the time evolution of the multi-model mean precipitation response (black line) by scaling the end-of century multi-model mean precipitation change based on the time-evolution of the mean ΔT (green line). Note that this is equivalent to repeating the procedure above,

but after setting i=0 in Equation 16. The pattern scaling (Figure 7b and Figure 7c) does not allow reproducing the multi-model mean change in Sahel precipitation from the 2000s to the 2030s, and particularly over the western Sahel (Figure 7b and Figure 7c). We suggest this to be due to the fact that the method does not account for the effects of global emissions in anthropogenic aerosols, which were shown to modulate Sahel precipitation over the historical period (e.*g.*, Herman et al. 2020; Monerie et al. 2022; Ndiaye et al. 2022). In addition, the difference between the simuated change in Sahel precipitation and the result of the pattern scaling can be due to changes in the spatial pattern in temperature change.

The pattern scaling approach gives similar results to the CMIP6 ensemble mean for the end of the 21st century. We then show that the A+M+ and A-M- scenarios alone largely capture the spread in western and central Sahel precipitation. Therefore, the storyline approach allows simulating the width of the CMIP6 uncertainty in Sahel precipitation change, as defined by the ensemble spread, after the mid-21st century (Figure 7b and Figure 7c). In other words, we further confirm that the two scenarios are not outliers, as compared to the responses obtained from each CMIP6 models within the transient SSP5-8.5 emission scenario (Figure 7b and Figure 7c).

4.4 Sensitivity to the North Atlantic and Euro-Mediterranean warming level

The results obtained up to now have used a fixed value for the scenario index (*e.g.*, i=1.46 for A+M/A-M-). The values of the scenario index dictates the intensity of the change in North Atlantic and Euro-Mediterranean temperature, and can thus have strong effects on future changes in Sahel precipitation. We test the sensitivity to the scenario index by computing changes in western and central Sahel precipitation, based on $\Delta V_x = \Delta T[a_x + i(b_x + c_x)]$, with the scenario index ranging between -2 and +2. We computed changes in precipitation for each grid point before evaluating the western and central Sahel precipitation indices. A scenario index of +1.46 yields the same changes in precipitation as in A+M+ and a scenario index of -1.46 yields the same changes in precipitation as in A-M- (Equation 14 and Equation 15). We focus on the two scenarios that explain better the CMIP6 Sahel precipitation change uncertainty, that is A+M+ and A-M-, and we do not assess the sensitivity to the scenario index for A+M- and A-M+.

Figure 8 shows how changes in western and central Sahel precipitation are sensitive to combinations of changes in global mean surface air temperature and the scenario index. The sign of the change in western Sahel precipitation is highly sensitive to the value of the scenario index, with a negative value of *i* and a positive value of *i* leading to an increase and a decrease in precipitation, respectively (Figure 8a). The multi-model mean prediction of no change in precipitation (scenario index=0) needs to be seen with caution since both wetting and drying are plausible depending on the amount of warming in the North atlantic and Euro-Mediterranean regions. Over the central Sahel, the likelihood of having an increase in precipitation is high as only with a strong negative value of *i* it is expected a slight decrease in precipitation (Figure 8b). Higher global-mean warming typically drives a larger wetting, but the uncertainty associated with the scenario index is substantial.

5. Mechanisms in selected CMIP6 models

We show the time evolution of the changes in the western (Figure 9a) and central (Figure 9b) Sahel precipitation, in function of ΔT, for all individual models. We then assess effects of the A+M+ and A-M- scenarios within the CMIP6 ensemble, selecting models that are showing higher and lower than average warmings of the North Atlantic and Euro-Mediterranean areas. The two new ensembles are

also useful to analyse mechanisms that explain changes in Sahel precipitation. We hereafter refer to as the A+M+ models, the models that lie on the quadrants of A+M+ and that are outside of the inner ellipse (Fig. 5). The A-M- models are the models that lie on the quadrants of A-M- and that are outside of the inner ellipse. We show that the A+M+ models reproduce an increase in Sahel precipitation that is stronger than the multi-model mean, while the A-M- models simulate less precipitation than the multi-model mean towards high values in ΔT (Figure 9a and Figure 9b).

There is a clear separation between the A+M+ and A-M- ensembles for a ΔT of 2.5-3K, showing that both groups of models are associated with different changes in precipitation (see the bars on Figure 5). These results confirm that the rate of warming of the Euro-Mediterranean area and of the North Atlantic Ocean, relative to the global mean increase in surface air temperature, can explain a large proportion of the uncertainty in Sahel precipitation change, for high values in ΔT (or, in other words, for the end of the 21st century).

The spread in precipitation change associated with a shift of the atmospheric circulation (ΔP_{shift}) is nearly identical to the one obtained for the total precipitation change, showing a strong control of shift of the atmospheric circulation on Sahel precipitation change uncertainty (Figure 9c and Figure 9d) within the CMIP6 ensemble, as shown in Monerie et al. (2020b). This is further confirmed by the A+M+ and A-M- models that show the same behaviour for the change in both central and western Sahel precipitation (Figure 9a and Figure 9b) and for ΔP_{shift} (Figure 9c and Figure 9d). This is also consistent with the effects of a warming of the North Atlantic SSTs, that primarily affect Sahel precipitation through dynamic changes of the circulation (Monerie et al. 2019).

We show that the change in the mean tropical circulation is less uncertain, with no strong differences between A+M+ and A-M- models in future changes in ΔP_{weak} (Figure S2). The same conclusion is drawn for ΔP_{therm} (Figure S3).

Uncertainty in Sahel precipitation change is therefore strongly associated with effects of the remote drivers on the shift of the monsoon circulation. As stated in the introduction, a northward shift of the monsoon system is accompanied by a northward shift in the location of the Saharan Heat Low. The SHL moves northwards due to the warming of northern Africa, but the northward shift of the SHL is substantially stronger in the A+M+ models than in the A-M- models (Figure 9e).

We note that the northward shift of the SHL in A-M- models may seems unconsistent with a decrease in precipitation over the western Sahel in A-M- models (Figure 8a). We suggest the decrease in western Sahel precipitation in A-M- models to be due to the weaker warming of the North Atlantic SSTs relative to the warming of the tropical SSTs (Figure S4), leading to a southward shift of the ITCZ over the tropical Atlantic and western West Africa (Monerie et al. 2021). In addition, the warming of the tropical SSTs leads to an increase in vertical static stability over the tropics (Gaetani et al. 2017; Hill et al. 2017; Monerie et al. 2021), which directly inhibits the future increase in precipitation. This is particularly relevant here because the effect of a warming of the tropical SSTs was shown to be particularly strong over the western Sahel within the CMIP6 ensemble (Gaetani et al. 2017; Monerie et al. 2020a).

6. Summary and discussion

A high inter-model spread in the simulated changes in Sahel precipitation lowers our confidence in the projections. Uncertainties in Sahel precipitation were shown to derive from uncertain projection of atmospheric circulation patterns (Monerie et al. 2020b). In this study we use a storyline approach previously applied to extratropical circulation changes (Zappa et Shepherd 2017, Mindlin et al. 2020)

to further investigate the role of remote sources of uncertainty on the Sahel precipitation and the monsoon circulation.

We show that changes in North Atlantic and in Euro-Mediterranean temperatures explain up to 50% of the central Sahel precipitation change uncertainty. We expect some of the processes controlling the uncertainty in changes in the North Atlantic SSTs to be different to the processes controlling the uncertainty in changes in Euro-Mediterraenan temperature. We then assume the selection of the two remote drivers to sample a large range of sources of climate change uncertainty. Uncertainty in future changes of the Atlantic meridional overturning circulation has strong effects on future changes in North Atlantic temperature (Bellomo et al. 2021; Swingedouw et al. 2021) while uncertainty in local land/cloud feedback rather strongly contribute to the uncertainty in surface air temperature change over Southern Europe (Boé et Terray 2014), and thus possibly the Mediterranean Sea.

Based on these remote sources of uncertainty, we constructed four different scenarios. In the A+M+ scenario, a concomitant anomalously high increase in temperature of the North Atlantic Ocean and Euro-Mediterranean area promotes a northward shift of the Atlantic ITCZ and of the West African monsoon, increasing precipitation in both the central and western Sahel. The dynamic shift of the monsoon system is accompanied by a northward shift of the Saharan Heat Low that allows strengthening low-level westerlies and increasing central Sahel precipitation. In contrast to A+M+, the A-M- scenario (small warming over both the North Atlantic and the Euro-Mediterranean temperature) is associated with a decrease in western Sahel precipitation and a smaller change in central Sahel precipitation than the multi model mean. We attribute the change in precipitation of the A-M- scenario to a cooling of the North Atlantic Ocean relative to the tropics, and to a southward shift of the ITCZ over the Atlantic Ocean and West Africa.

Interestingly, in the A+M- scenario, the effects of an anomalously large increase in North Atlantic Ocean temperature counterbalance those of an anomalously low increase in Euro-Mediterranean temperature on both the western and central Sahel precipitation, showing that both oceanic basins have a similar effect on uncertainty in Sahel precipitation change. Likewise, the A-M+ scenario also shows a cancelation of effects across the Sahel.

We use the outputs of the Storyline approach to provide a method that could be helpful at selecting models for impacts studies: by selecting models based on their sensitivity to climate change over the North Atlantic and Mediterranean Sea, one can sample a large range of uncertainty in Sahel precipitation change with just few models. This method has the advantage of allowing a focus on the physical mechanisms of change in the selected models. For instance, one can address the effect of an uncertain warming of the Mediterranean Sea and the North Atlantic Ocean on future changes in precipitation extremes, dry spells, or monsoon onset, among others. This approach is therefore complementary to others that are based on patterns in precipitation change (Monerie et al. 2016) or detailed analyses of model biases (McSweeney et al. 2015).

A limitation of the study is that the storyline approach (Zappa et Shepherd 2017) relies on a statistical analysis across the CMIP6 ensemble. We argue that a mechanistic approach should therefore also be used to assess how uncertainty in the remote drivers can lead to uncertainty in Sahel precipitation change. In future work, a first step could be achieved by prescribing SST anomalies, derived from the A+M+ and A-M- scenarios, in AMIP-type simulations. In addition to anomalies in SST, experiments could include difference in physics of the dust particles (e.g., absorption properties) and of simulation of the vegetation-atmosphere feedbacks. This will help understanding better the mechanism for which uncertain changes in extratropical SSTs can lead to uncertainty in Sahel precipitation change.

We acknowledge that in addition to changes in SSTs, uncertainty in Sahel precipitation change can also be due to (i) differences between models at simulating the amount of atmospheric mineral dust (Zhao et al. 2022) and its direct effects on the West African monsoon system (Solmon et al. 2008;

Evan et al. 2016), (ii) effects of changes in vegetation cover (Wang et Alo 2012) and land-atmosphere feedbacks (Koster et al. 2004), or (iii) effects of changes in anthropogenic aerosols on Sahel precipitation (Monerie et al. 2023). (iv) Differences in model's convective schemes are also strong sources of uncertainty (Ramarohetra et al. 2015; Yan et al. 2018). Moreover, feedbacks between changes in subtropical temperature and mineral dust amounts or vegetation cover over West Africa, through changes in wind speed, temperature, and precipitation could be a strong source of uncertainty in the Earth System Models of the CMIP6 ensemble. Further work could focus on assessing these other sources of uncertainty for Sahel precipitation change.

Ackonwledgements

We acknowledge the World Climate Research Programme, which, through its Working Group on Coupled Modelling, coordinated and promoted CMIP6. We thank the climate modeling groups for producing and making available their model output, the Earth System Grid Federation (ESGF) for archiving the data and providing access, and the multiple funding agencies who support CMIP6 and ESGF. J.M. was supported by ANR-19-JPOC-003 JPI climate/JPI ocean ROADMAP and by the ARCHANGE project of the "Make our planet great again" program (ANR-18-MPGA-0001, France). EM acknowledges the funding provided by the Spanish Ministry of Science and Competitiveness DISTROPIA (PID2021-125806NB-I00) project. G. Z. acknowledges funding from the Italian Ministry of Education, University and Research (MIUR) through the JPI Oceans/Climate ROADMAP Project (D. M. 593/2016).

Data availability statement

CMIP6 GCM output is available from public repositories, including https://esgf-index1.ceda.ac.uk/search/cmip6-ceda/.

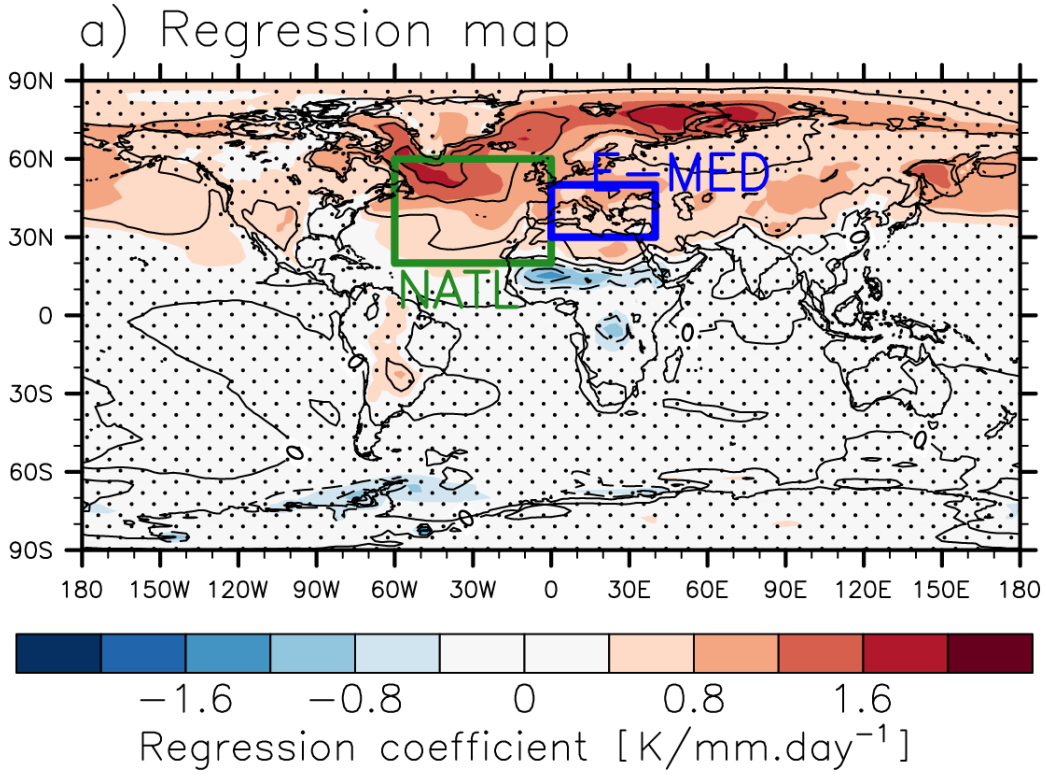

Figure 1: Regression coefficients [K/mm.d^{-1}], between changes in Sahel precipitation (central Sahel precipitation in colour and western Sahel precipitation with contours), across the CMIP6 ensemble (See Table 1). Contours range from -2 to +2, every 0.5 K/mm.d^{-1}. Stippling indicates that the regression coefficient is not significant at the 5% level according to a Student's *t* test, for the central Sahel. The green box indicates the area that was used to compute the NATL index and the blue box indicates the area that was used to compute the Euro-Mediterranean index.

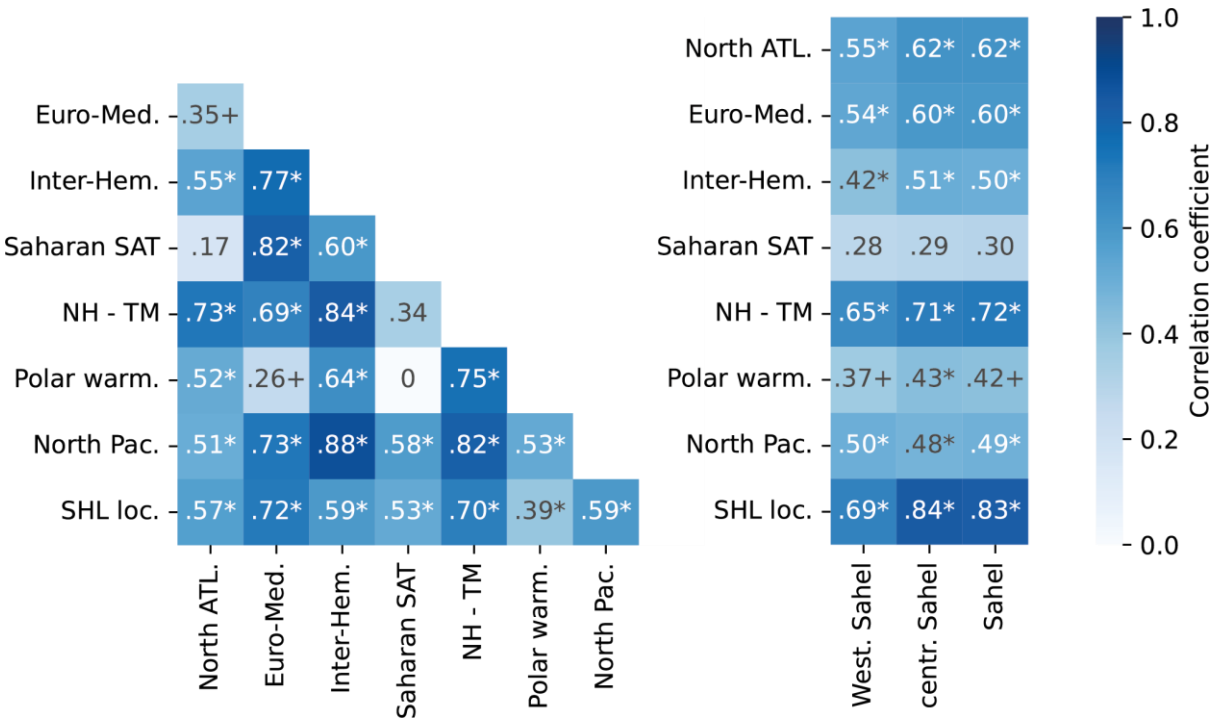

Figure 2: (Left) Correlation coefficient between the projected changes in height climate indices, here selected as possible drivers of Sahel precipitation, scaled by ΔT across CMIP6 models. (Right) Correlation coefficient between the projected changes in the climate indices and the change in the western, central and entire Sahel (10°W-10°E) precipitation, across CMIP6 models. A star (plus) indicates that the correlation coefficient is significant at the 1% (5%) level. North ATL stands for North Atlantic Ocean temperature, Euro-Med is the temperature averaged over the Euro-Mediterraean area, Inter-Hem is the inter-hemispheric temperature gradient, Saharan SAT is for the temperature averaged over the Sahara desert, NH-TM is the northern hemisphere temperature relative to the tropics, Polar warm stands for the polar amplification, North Pac is the temperature averaged over the northern Pacific Ocean. SHL loc is for the location (°North) of the Saharan Heat Low. See section 2.2.2 for the definition of the indices.

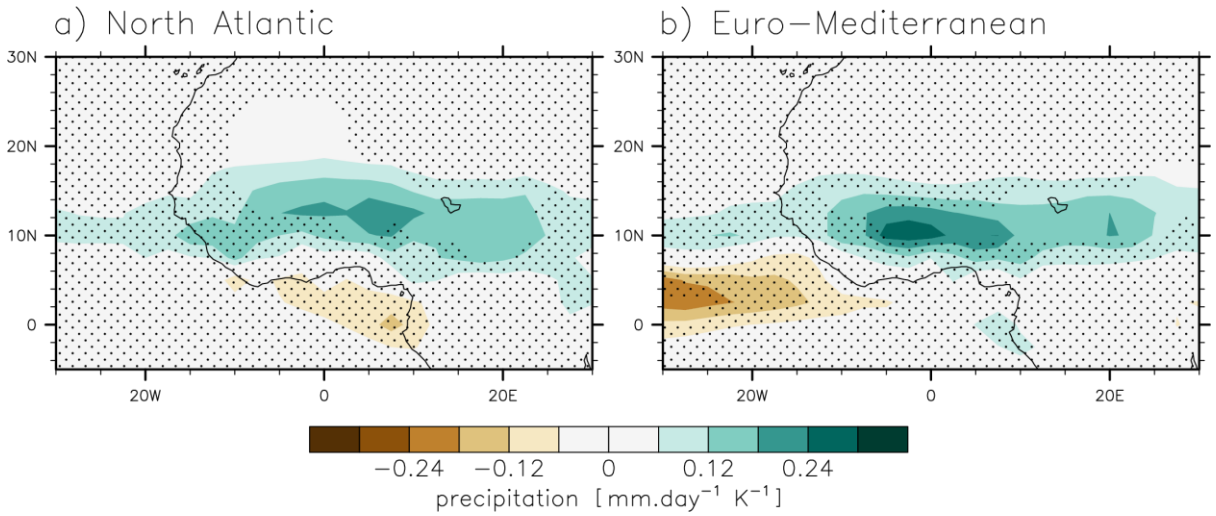

Figure 3: Sensitivity of the projected changes in precipitation [mm.day^{-1} K^{-1}] to the uncertainty in the magnitude of the (a) North Atlantic warming (b_x) and of (b) the Euro-Mediterranean warming (c_x). b_x and c_x are estimated with a multiple linear regression framework, following Equation (3). Stippling indicates that regression values are not significant at the 5% level according to a Student's *t* test.

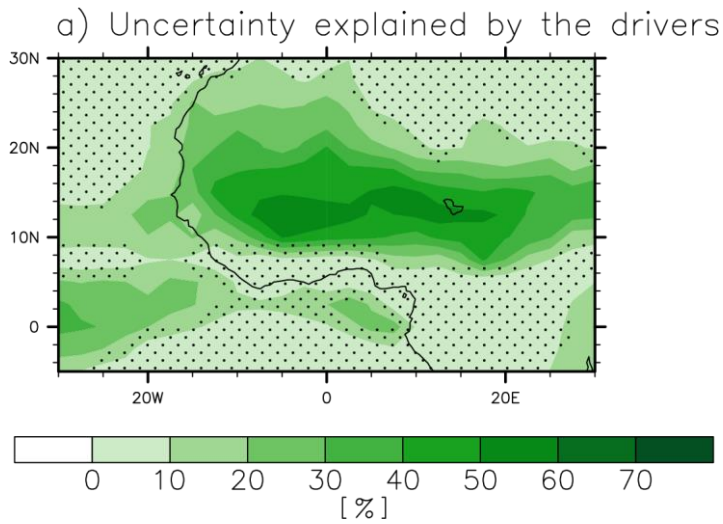

Figure 4: Fraction of the uncertainty in the precipitation response to climate change that is explained by the uncertainty in the response of the remote drivers and by global warming (r^2 defined from the CMIP6 inter-model spread and $\Delta T_m[a_x + b_x(\frac{\Delta T_{NATL}}{\Delta T})'_m + c_x(\frac{\Delta T_{MED}}{\Delta T})'_m]$) (from equation 3) at the end of the 21st century. Stippling indicates where the correlation coefficient is not significant at the 5% level.

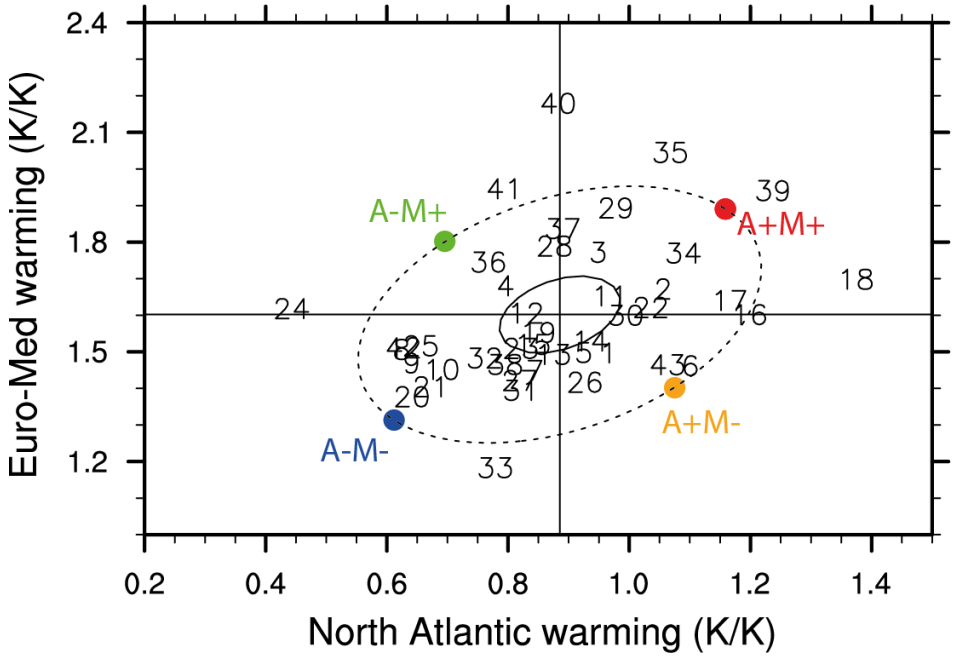

Figure 5: Changes in Euro-Mediterranean temperature ($\frac{\Delta T_{MED}}{\Delta T}$) and North Atlantic temperature ($\frac{\Delta T_{NATL}}{\Delta T}$), scaled by global-mean warming (K.K^{-1}). Each CMIP6 model is shown by its number (See Table S1). The inner ellipse delimitates models that have low anomalies relative to the multi-model mean, i.e. when the combined standardized anomaly in the driver response is smaller than 0.5. *e.g.*, $\sqrt{[(\frac{\Delta T_{NATL}}{\Delta T})'_m]^2 - 2r\,(\frac{\Delta T_{NATL}}{\Delta T})'_m(\frac{\Delta T_{MED}}{\Delta T})'_m + [(\frac{\Delta T_{MED}}{\Delta T})'_m]^2} < 0.5$, following (Mindlin et al. 2020). Vertical and horizontal lines denote the multi-model mean changes in Euro-Mediterranean and North Atlantic temperature. The outer ellipse marks the 80% confidence region of the CMIP6 model distributions, assuming the responses in the two drivers follow a bivariate normal distribution with an across-model correlation coefficient between $\frac{\Delta T_{NATL}}{\Delta T}$ and $\frac{\Delta T_{MED}}{\Delta T}$ equal to 0.35 . The four storylines (A+M+, A-M-, A+M-, A-M+) are selected on the confidence ellipse so that they reflect equal standardized anomalies in each driver (see supplementary material for details).

-

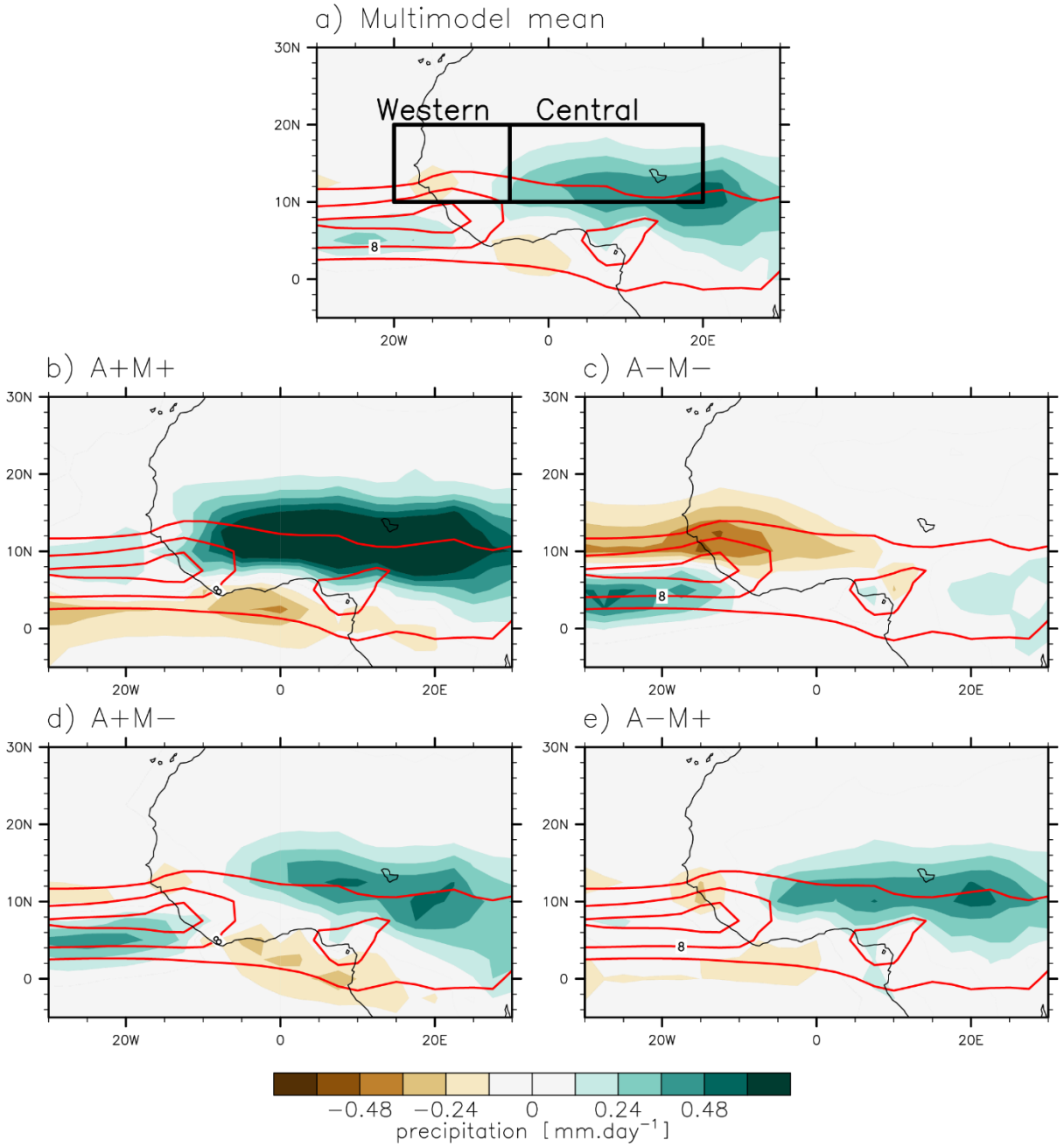

Figure 6: Changes in precipitation scaled by ΔT [mm.day^{-1}.K^{-1}] for the end of the 21st century and for the (a) multi model mean (SSP5.8-5 minus historical simulations) and the four scenarios (b) A+M+, (c) A-M-, (d) A+M- and (e) A-M+. The black boxes in Figure 5a show the areas that were used to define the western and central Sahel precipitation indices. Red contours indicate the climatological precipitation in JAS over 1960-1999 for the CMIP6 ensemble mean (historical simulations).

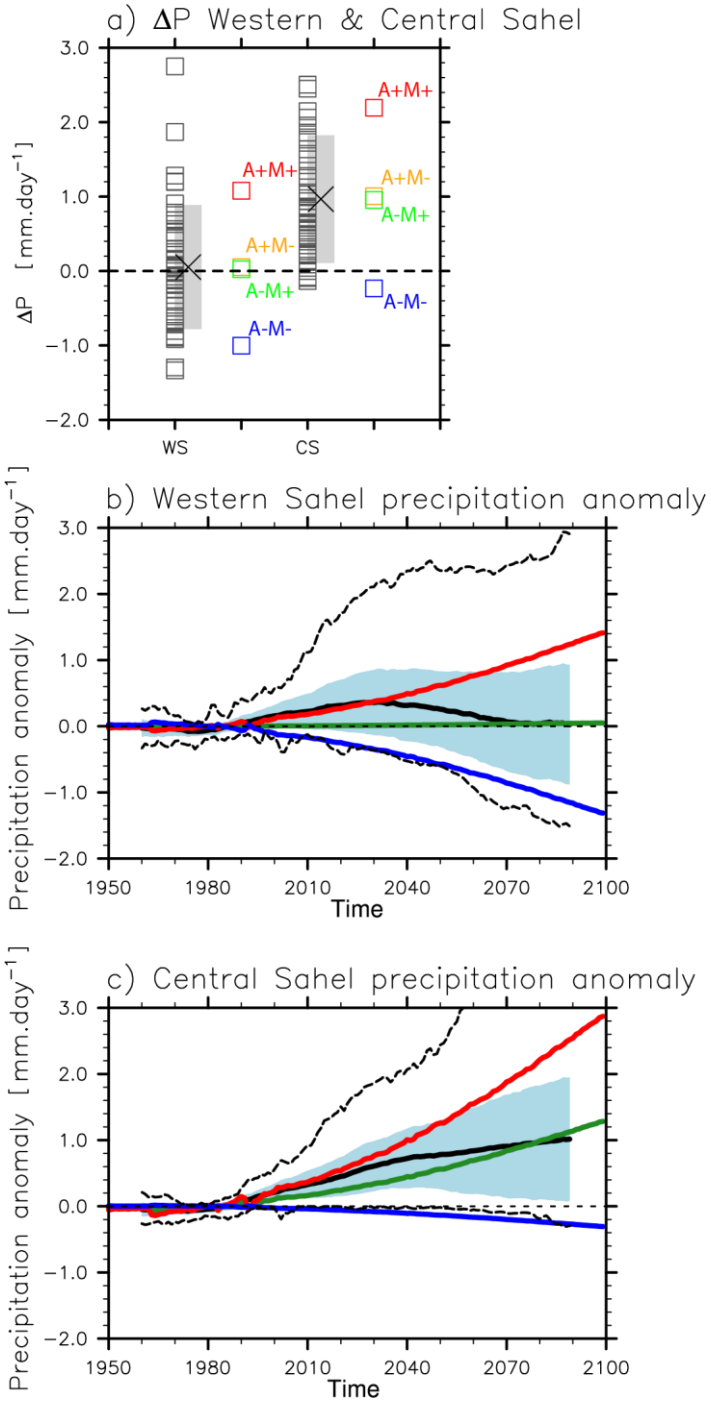

Figure 7: (a) Changes in central and western Sahel precipitation for each CMIP6 model (black) and the four scenarios (colours) at the end of the 21st century. The CMIP6 ensemble mean is shown with a black cross and the multi model mean plus and minus one standard deviation by the grey shading. Changes in (b) western and (c) central Sahel precipitation for the CMIP6 ensemble mean (black), the pattern scaling method on SSP5-8.5 changes in precipitation (green), and the A+M+ (red) and A-M- (blue) scenarios. The CMIP6 spread (multi model mean plus and minus one standard deviation) is shown by the blue shading. Dotted lines show the maximum and minimum values in precipitation anomaly across the CMIP6 ensemble. A 21-year running mean was applied to filter out the high frequency variability for the CMIP6 models. Anomalies are relative to the 1960-1999 period.

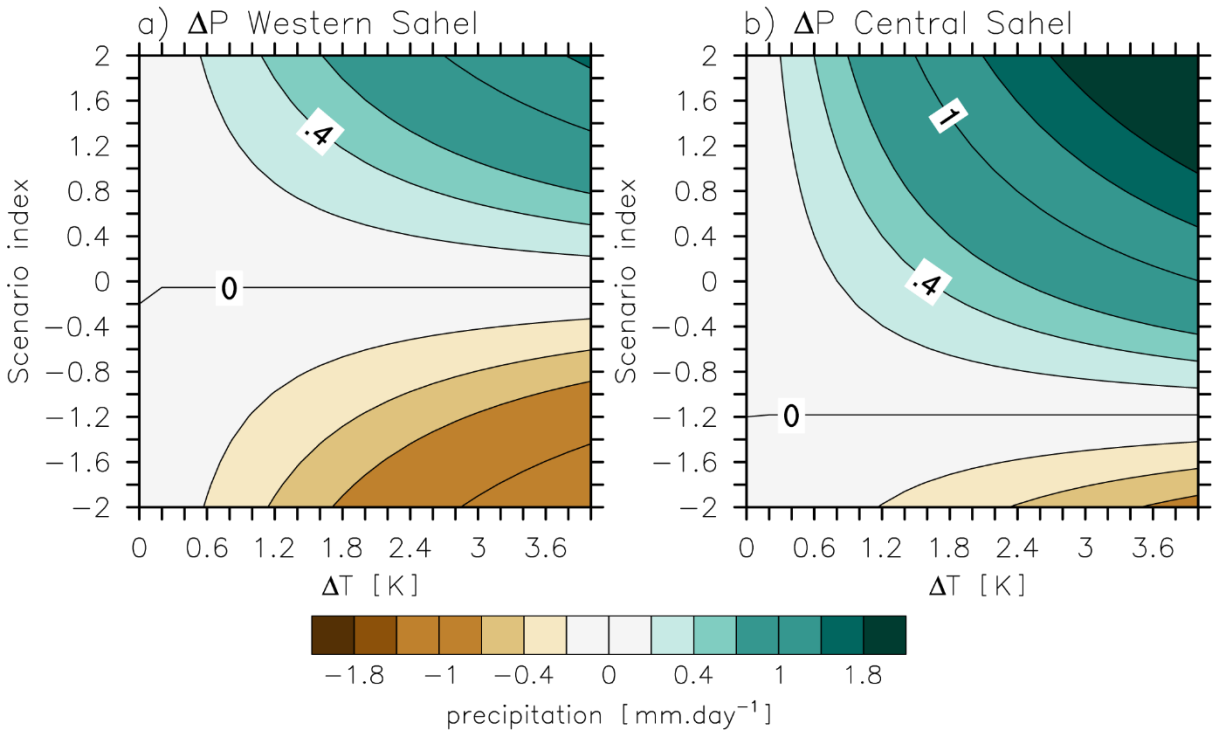

Figure 8: Changes in (a) western and (b) central Sahel precipitation [mm.d^{-1}], in function of the scenario index (see text for detail) and of the magnitude of changes in global mean surface air temperature (ΔT).

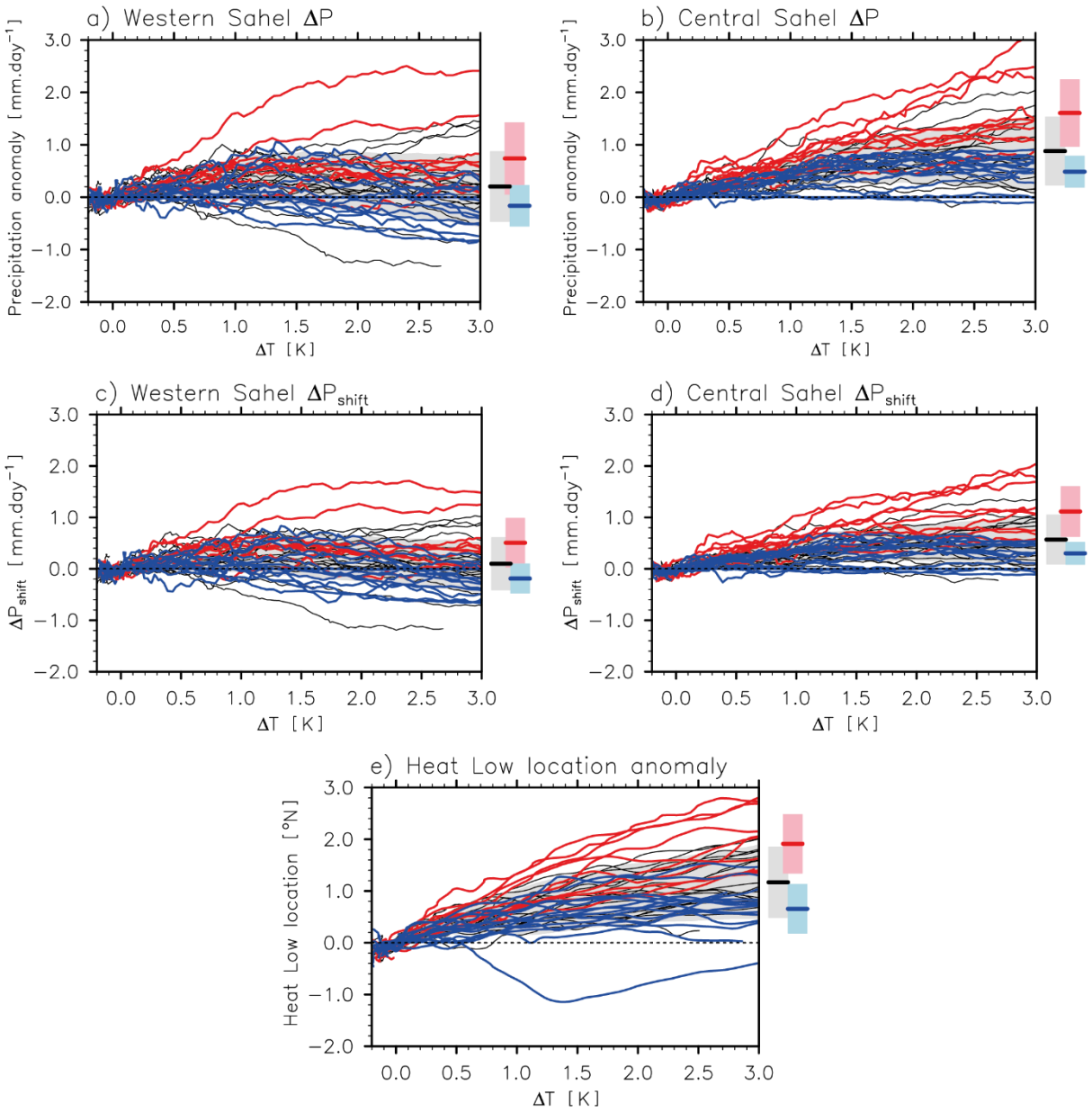

Figure 9: Changes in (a) western and (b) central Sahel precipitation [mm.day^{-1}] in function of the warming (ΔT) for all models (black lines) and CMIP6 envelope (grey shading, spanning 2 times the CMIP6 standard deviation), the A+M+ models (red), the A-M- models (blue). (c) and (d), as in (a) and (b) but for ΔP_{shift}. (e) Changes in the latitudinal location of the Saharan Heat low (°N). On the right hand side of each panel, the horizontal thick lines indicate the ensemble mean, and the bars is the ensemble envelope (spanning 2 times the ensemble standard deviation), computed across the CMIP6 models (black), the A+M+ models (red) and the A-M- models (blue), for a warming of 2.5-3°C.

References

Baarsch F, Granadillos JR, Hare W, et al (2020) The impact of climate change on incomes and convergence in Africa. World Dev 126:104699 . doi: https://doi.org/10.1016/j.worlddev.2019.104699

Bellomo K, Angeloni M, Corti S, von Hardenberg J (2021) Future climate change shaped by inter-model differences in Atlantic meridional overturning circulation response. Nat Commun 12:3659 . doi: 10.1038/s41467-021-24015-w

Biasutti M (2013a) Forced Sahel rainfall trends in the CMIP5 archive. J Geophys Res Atmos 118:1613-1623 . doi: 10.1002/jgrd.50206

Biasutti M (2013b) Forced Sahel rainfall trends in the CMIP5 archive. J Geophys Res Atmos 118:1613-1623 . doi: 10.1002/jgrd.50206

Biasutti M, Held IM, Sobel AH, Giannini A (2008) SST Forcings and Sahel Rainfall Variability in Simulations of the Twentieth and Twenty-First Centuries. J Clim 21:3471-3486 . doi: 10.1175/2007JCLI1896.1

Biasutti M, Sobel AH, Camargo SJ (2009) The Role of the Sahara Low in Summertime Sahel Rainfall Variability and Change in the CMIP3 Models. J Clim 22:5755-5771 . doi: 10.1175/2009JCLI2969.1

Boé J, Terray L (2014) Land–sea contrast, soil-atmosphere and cloud-temperature interactions: interplays and roles in future summer European climate change. Clim Dyn 42:683-699 . doi: 10.1007/s00382-013-1868-8

Chadwick R, Boutle I, Martin G (2013) Spatial Patterns of Precipitation Change in CMIP5: Why the Rich Do Not Get Richer in the Tropics. J Clim 26:3803-3822 . doi: 10.1175/JCLI-D-12-00543.1

Chadwick R, Good P, Willett K (2016) A Simple Moisture Advection Model of Specific Humidity Change over Land in Response to SST Warming. J Clim 29:7613-7632 . doi: 10.1175/JCLI-D-16-0241.1

Cissé G (2019) Food-borne and water-borne diseases under climate change in low- and middle-income countries: Further efforts needed for reducing environmental health exposure risks. Acta Trop 194:181-188 . doi: https://doi.org/10.1016/j.actatropica.2019.03.012

Dong B, Sutton R (2015) Dominant role of greenhouse-gas forcing in the recovery of Sahel rainfall. Nat Clim Chang 5:757-760 . doi: 10.1038/nclimate2664

Evan AT, Flamant C, Gaetani M, Guichard F (2016) The past, present and future of African dust. Nature 531:493-495 . doi: 10.1038/nature17149

Eyring V, Bony S, Meehl GA, et al (2016) Overview of the Coupled Model Intercomparison Project Phase 6 (CMIP6) experimental design and organization. Geosci Model Dev 9:1937-1958 . doi: 10.5194/gmd-9-1937-2016

Fontaine B, Garcia-Serrano J, Roucou P, et al (2010) Impacts of warm and cold situations in the Mediterranean basins on the West African monsoon: observed connection patterns (1979--2006) and climate simulations. Clim Dyn 35:95-114 . doi: 10.1007/s00382-009-0599-3

Gaetani M, Flamant C, Bastin S, et al (2017) West African monsoon dynamics and precipitation: the competition between global SST warming and CO2 increase in CMIP5 idealized simulations. Clim Dyn 48:1353-1373 . doi: 10.1007/s00382-016-3146-z

Giannini A, Salack S, Lodoun T, et al (2013) A unifying view of climate change in the Sahel linking intra-seasonal, interannual and longer time scales. Environ Res Lett 8:24010 . doi:

10.1088/1748-9326/8/2/024010

Held IM, Soden BJ (2006) Robust Responses of the Hydrological Cycle to Global Warming. J Clim 19:5686-5699 . doi: 10.1175/JCLI3990.1

Herman RJ, Giannini A, Biasutti M, Kushnir Y (2020) The effects of anthropogenic and volcanic aerosols and greenhouse gases on twentieth century Sahel precipitation. Sci Rep 10:12203 . doi: 10.1038/s41598-020-68356-w

Hill SA, Ming Y, Held IM, Zhao M (2017) A Moist Static Energy Budget–Based Analysis of the Sahel Rainfall Response to Uniform Oceanic Warming. J Clim 30:5637-5660 . doi: 10.1175/JCLI-D-16-0785.1

Hirasawa H, Kushner PJ, Sigmond M, et al (2020) Anthropogenic aerosols dominate forced multidecadal Sahel precipitation change through distinct atmospheric and oceanic drivers. J Clim 1-56 . doi: 10.1175/JCLI-D-19-0829.1

Jankowska MM, Lopez-Carr D, Funk C, et al (2012) Climate change and human health: Spatial modeling of water availability, malnutrition, and livelihoods in Mali, Africa. Appl Geogr 33:4-15 . doi: https://doi.org/10.1016/j.apgeog.2011.08.009

Koster RD, Dirmeyer PA, Guo Z, et al (2004) Regions of Strong Coupling Between Soil Moisture and Precipitation. Science (80-) 305:1138 LP - 1140 . doi: 10.1126/science.1100217

Lavaysse C, Flamant C, Evan A, et al (2016) Recent climatological trend of the Saharan heat low and its impact on the West African climate. Clim Dyn 47:3479-3498 . doi: 10.1007/s00382-015-2847-z

Lavaysse C, Flamant C, Janicot S, et al (2009) Seasonal evolution of the West African heat low: a climatological perspective. Clim Dyn 33:313-330 . doi: 10.1007/s00382-009-0553-4

Liu Y, Chiang JCH, Chou C, Patricola CM (2014) Atmospheric teleconnection mechanisms of extratropical North Atlantic SST influence on Sahel rainfall. Clim Dyn 43:2797-2811 . doi: 10.1007/s00382-014-2094-8

Manzini E, Karpechko AY, Anstey J, et al (2014) Northern winter climate change: Assessment of uncertainty in CMIP5 projections related to stratosphere-troposphere coupling. J Geophys Res Atmos 119:7979-7998 . doi: https://doi.org/10.1002/2013JD021403

Marega O, Mering C, Meunier V (2018) Sahelian agro-pastoralists in the face of social and environmental changes: New issues, new risks, new transhumance axe. Lesp Geogr 47:235-260

Martin ER, Thorncroft CD (2014) The impact of the AMO on the West African monsoon annual cycle. Q J R Meteorol Soc 140:31-46 . doi: 10.1002/qj.2107

Marvel K, Biasutti M, Bonfils C (2020) Fingerprints of external forcing agents on Sahel rainfall: aerosols, greenhouse gases, and model-observation discrepancies. Environ Res Lett 15:084023

McSweeney CF, Jones RG, Lee RW, Rowell DP (2015) Selecting CMIP5 GCMs for downscaling over multiple regions. Clim Dyn 44:3237-3260 . doi: 10.1007/s00382-014-2418-8

Mindlin J, Shepherd TG, Vera CS, et al (2020) Storyline description of Southern Hemisphere midlatitude circulation and precipitation response to greenhouse gas forcing. Clim Dyn 54:4399-4421 . doi: 10.1007/s00382-020-05234-1

Mohino E, Janicot S, Bader J (2011) Sahel rainfall and decadal to multi-decadal sea surface temperature variability. Clim Dyn 37:419-440 . doi: 10.1007/s00382-010-0867-2

Monerie P-A, Dittus AJ, Wilcox LJ, Turner AG (2023) Uncertainty in Simulating Twentieth Century West African Precipitation Trends: The Role of Anthropogenic Aerosol Emissions. Earth's Futur 11:e2022EF002995 . doi: https://doi.org/10.1029/2022EF002995

Monerie P-A, Pohl B, Gaetani M (2021) The fast response of Sahel precipitation to climate change allows effective mitigation action. npj Clim Atmos Sci 4:24 . doi: 10.1038/s41612-021-00179-6

Monerie P-A, Robson J, Dong B, et al (2019) Effect of the Atlantic Multidecadal Variability on the Global Monsoon. Geophys Res Lett 46: . doi: 10.1029/2018GL080903

Monerie P-A, Sanchez-Gomez E, Boé J (2016) On the range of future Sahel precipitation projections and the selection of a sub-sample of CMIP5 models for impact studies. Clim Dyn. doi: 10.1007/s00382-016-3236-y

Monerie P-A, Sanchez-Gomez E, Gaetani M, et al (2020a) Future evolution of the Sahel precipitation zonal contrast in CESM1. Clim Dyn. doi: 10.1007/s00382-020-05417-w

Monerie P-A, Wainwright CM, Sidibe M, Akinsanola AA (2020b) Model uncertainties in climate change impacts on Sahel precipitation in ensembles of CMIP5 and CMIP6 simulations. Clim Dyn 55:1385-1401 . doi: 10.1007/s00382-020-05332-0

Monerie P-A, Wilcox LJ, Turner AG (2022) Effects of anthropogenic aerosol and greenhouse gas emissions on Northern Hemisphere monsoon precipitation: mechanisms and uncertainty. J Clim 1-66 . doi: 10.1175/JCLI-D-21-0412.1

Mutton H, Chadwick R, Collins M, et al (2022) The Impact of the Direct Radiative Effect of Increased CO2 on the West African Monsoon. J Clim 35:2441-2458 . doi: 10.1175/JCLI-D-21-0340.1

Ndiaye CD, Mohino E, Mignot J, Sall SM (2022) On the detection of externally-forced decadal modulations of the Sahel rainfall over the whole 20th century in the CMIP6 ensemble. J Clim 1-51 . doi: 10.1175/JCLI-D-21-0585.1

O'Neill BC, Tebaldi C, van Vuuren DP, et al (2016) The Scenario Model Intercomparison Project (ScenarioMIP) for CMIP6. Geosci Model Dev 9:3461-3482 . doi: 10.5194/gmd-9-3461-2016

Park J-Y, Bader J, Matei D (2015) Northern-hemispheric differential warming is the key to understanding the discrepancies in the projected Sahel rainfall. Nat Commun 6:5985

Park J, Bader J, Matei D (2016) Anthropogenic Mediterranean warming essential driver for present and future Sahel rainfall. Nat Clim Chang 6:941-945

Ramarohetra J, Pohl B, Sultan B (2015) Errors and uncertainties introduced by a regional climate model in climate impact assessments: example of crop yield simulations in West Africa. Environ Res Lett 10:124014 . doi: 10.1088/1748-9326/10/12/124014

Ramin BM, McMichael AJ (2009) Climate Change and Health in Sub-Saharan Africa: A Case-Based Perspective. Ecohealth 6:52 . doi: 10.1007/s10393-009-0222-4

Roehrig R, Chauvin F, Lafore J-P (2011) 10–25-Day Intraseasonal Variability of Convection over the Sahel: A Role of the Saharan Heat Low and Midlatitudes. J Clim 24:5863-5878 . doi: 10.1175/2011JCLI3960.1

Rowell DP (2003) The Impact of Mediterranean SSTs on the Sahelian Rainfall Season. J Clim 16:849-862 . doi: 10.1175/1520-0442(2003)016<0849:TIOMSO>2.0.CO;2

Sainte Fare Garnot V, Groth A, Ghil M (2018) Coupled Climate-Economic Modes in the Sahel's Interannual Variability. Ecol Econ 153:111-123 . doi: https://doi.org/10.1016/j.ecolecon.2018.07.006

Sanogo S, Fink AH, Omotosho JA, et al (2015) Spatio-temporal characteristics of the recent rainfall recovery in West Africa. Int J Climatol 35:4589-4605 . doi: 10.1002/joc.4309

Schneider T, Bischoff T, Haug GH (2014) Migrations and dynamics of the intertropical convergence zone. Nature 513:45

Shekhar R, Boos WR (2017) Weakening and Shifting of the Saharan Shallow Meridional Circulation during Wet Years of the West African Monsoon. J Clim 30:7399-7422 . doi: 10.1175/JCLI-D-16-0696.1

Solmon F, Mallet M, Elguindi N, et al (2008) Dust aerosol impact on regional precipitation over western Africa, mechanisms and sensitivity to absorption properties. Geophys Res Lett 35: . doi: https://doi.org/10.1029/2008GL035900

Sultan B, Gaetani M (2016) Agriculture in West Africa in the Twenty-First Century: Climate Change and Impacts Scenarios, and Potential for Adaptation. Front Plant Sci 7:1262 . doi: 10.3389/fpls.2016.01262

Swingedouw D, Bily A, Esquerdo C, et al (2021) On the risk of abrupt changes in the North Atlantic subpolar gyre in CMIP6 models. Ann N Y Acad Sci 1504:187-201 . doi: https://doi.org/10.1111/nyas.14659

Taylor KE, Stouffer RJ, Meehl GA (2012) An overview of CMIP5 and the experiment design. Bull. Am. Meteorol. Soc. 93:485-498

Wang G, Alo CA (2012) Changes in precipitation seasonality in West Africa predicted by RegCM3 and the impact of dynamic vegetation feedback. Int J Geophys 2012:

Yan Y, Lu R, Li C (2018) Relationship between the Future Projections of Sahel Rainfall and the Simulation Biases of Present South Asian and Western North Pacific Rainfall in Summer. J Clim 32:1327-1343 . doi: 10.1175/JCLI-D-17-0846.1

Zappa G, Shepherd TG (2017) Storylines of Atmospheric Circulation Change for European Regional Climate Impact Assessment. J Clim 30:6561-6577 . doi: 10.1175/JCLI-D-16-0807.1

Zhao A, Ryder CL, Wilcox LJ (2022) How well do the CMIP6 models simulate dust aerosols? Atmos Chem Phys 22:2095-2119 . doi: 10.5194/acp-22-2095-2022